A reduced model of pulsatile flow in an arterial compartment

Emmanuelle Crépeau, Michel Sorine

A reduced model of pulsatile flow in an arterial compartment.

Emmanuelle Crépeau and Michel Sorine

Université de Versailles-Saint Quentin en Yvelines, 78000 Versailles
crepeau@math.uvsq.fr
INRIA, Projet SOSSO,
Domaine de Voluceau-Rocquencourt, 78153 Le Chesnay Cedex
Michel.Sorine@inria.f

Abstract

In this article we propose a reduced model of the input-output behaviour of an arterial compartment, including the short systolic phase where wave phenomena are predominant. The objective is to provide basis for model-based signal processing methods for the estimation from non-invasive measurements and the interpretation of the characteristics of these waves. Due to phenomena such that peaking and steepening, the considered pressure pulse waves behave more like solitons generated by a Korteweg de Vries (KdV) model than like linear waves. So we start with a quasi-1D Navier-Stokes equation taking into account radial acceleration of the wall : the radial acceleration term being supposed small, a multiscale singular perturbation technique is used to separate the fast wave propagation phenomena taking place in a boundary layer in time and space described by a KdV equation from the slow phenomena represented by a parabolic equation leading to two-elements windkessel models. Some particular solutions of the KdV equation, the 2 and 3-soliton solutions, seem to be good candidates to match the observed pressure pulse waves. Some very promising preliminary comparisons of numerical results obtained along this line with real pressure data are shown.

keywords: Modelisation, Korteweg-de Vries equation, windkessel model, solitons, pulsatile flow, arterial compartment.

1 Introduction

Reduced mathematical models of the cardiovascular system. The cardiovascular system can be seen as consisting of the heart, a complex

double chamber pump, pumping the blood into vessels organized into vascular compartments forming a closed circulation loop. This point of view is useful for building models of the whole system as interconnection of simpler subsystem models. Such reduced mathematical models are usually a set of coupled ordinary differential equations, each of them representing the input-output behaviour of a subsystem: conservation law of the blood quantity for short time-intervals and specific behaviour laws. They can be used for understanding the global hydraulic behaviour of the system during a heartbeat. They can also be used to study the short-term control by the autonomous nervous system [16, 14, 12].

Windkessel models of the input impedances of vascular compartments. Input-output models of vascular compartments are 0D models (differential equations with no space variable) used in the above-mentioned models of the cardiovascular system. Also called windkessel models, they have been intensively studied because they can be useful to define global characteristics of vascular compartments with a small number of parameters having a physiological meaning. The first results of this type go back to Stephen Hales [5] who measured blood pressure in a horse by inserting a tube into a blood vessel, allowing the blood to rise up the tube. Measuring the heart rate and the capacity of the left ventricle, he was able to estimate the output of the heart per minute, and then the resistance to flow of blood in the vessels, the ratio of the pressure over the flow. Considering the dynamical behaviour of pressure, led Otto Frank in 1899 [4] to propose the original two-element windkessel model to represent the seemingly exponential decay of pressure in the ascending aorta during diastole, when the input flow is zero. The time constant of this exponential decay is the product of the two elements of the model: the peripheral resistance, R_p, and the total arterial compliance, C. This model is analog to an electrical circuit, a two-port network with a parallel resistor R_p and a parallel input capacitor C. The input impedance is given by $Z_{in} = \frac{R_p}{1+j\omega R_p C}$. Since these first results, windkessel models with three or four elements have been introduced to represent more precisely the high-frequency behaviours of input impedances when it became possible to measure them [20]. The main observation leading to the three-element windkessel model is that the input impedance at high frequencies is close to a constant resistance R_c (constant modulus and zero degrees phase angle) that can be interpreted as the characteristic impedance of the compartment. The two-element model is then corrected as follows: $Z_{in} = R_c + \frac{R_p}{1+j\omega R_p C}$. But now, for low frequencies Z_{in} is close to $R_c + R_p$ instead of R_p, an error corrected by adding a fourth element, an inertance L in parallel with R_c, so that $Z_{in} = \frac{j\omega R_c L}{R_c+j\omega L} + \frac{R_p}{1+j\omega R_p C}$. Usually L is interpreted as the total inertance of the arterial system. Good estimations from aortic pressure and flow measurements, of the input impedance of the entire systemic tree, and in particular of the total arterial compliance have been

obtained using this four-element windkessel model [20].

Windkessel models and linear transmission line concepts. The linear transmission line theory is underlying the developments of windkessel models. The arterial systemic compartment can be seen as a multi-port network coupling the heart to the extremities of the arterial tree through series of vessel bifurcations. When modelling the aorta input impedance, three situations are considered [20]: for very low frequencies, the input impedance is close to the equivalent resistance R_p of the very distal parts of the arterial tree (arterioles and small arteries); for low frequencies the input impedance decreases due to the distributed compliance C and inertance L. Remark that $\frac{1}{\sqrt{LC}}$ is the wave velocity. Finally, for medium to high frequencies (above two times the heart rate), reflections in the proximal aorta can be neglected, so that, as in the case of a reflectionless line, the input impedance equals the characteristic impedance of the ascending aorta (a constant resistance for high frequencies). This reflectionless property does not seem to be limited to high frequencies. As noticed in [21]: " Indeed, Milnor [11] remarked that the properties of the aortic tree in the normal young animal are those of an almost perfect diffuser (i.e., it generates far fewer reflections than the best man-made distribution network)". We will come back on this property later. Estimating ascending aortic pressure from a distal pressure waveform is of particular interest in the case of a non-invasive distal measurement, for example for a distal pressure measured at the finger. Having in mind the linear transmission line concepts, the problem is to estimate an input-output transfer function between proximal and distal pressures. Several methods have been proposed ([6], [19]) but some important limitations appear when 0D models are used to represent the relations between distant signals [10]. This is not surprising because rational transfer functions have been used but the transmission line, in this case, behaves like a delay-line: an infinite dimensional system. We will propose a solution for this problem, based on some kind of nonlinear transmission line concepts.

Multiscale modelling of the cardiovascular system. Windkessel models are also used as models of the loads of the heart or of the arteries in some multiscale computations where they appear as boundary conditions of partial differential equations (PDE) when distributed models of the heart [1, 18] or of vessels [17] are used. In the case of vessel modelling, the question arises of the consistency of the lumped models with models taking into account one, two or three space variables to represent, apparently, the same vessels. It is discussed in [9] in the 1D case: a series of well chosen windkessel-like models can be used as a semi-discrete approximation of the linearized flow equations, while a single windkessel model can be used when it is possible to neglect the variations in space of pressure and flow (hypothesis (9) in [9]), a limitation that is not surprising for 0D models and seems valid after the pressure pulse wave has propagated through the arterial tree.

So windkessel models appear as low frequency approximations of the input impedances of the downstream compartments loading the studied element (heart or vessel). In [13], as a result of a direct spectral analysis of the linearized flow equations, the number of elements of the windkessel model is chosen in relation with the order of this low frequency approximation. These theoretical results are an explanation of the good experimental results reported for example in [20]. Remark that if one is interested by the transmission line transfer function, the approximation by a long series of winkessel models provided by this PDE approach is not a reduced model.

Reduced models of the arterial compartments based on nonlinear waves and windkessel models. In this article we propose reduced models of the input-output behaviour of vascular compartments, including the short systolic phase (about 100 ms) where wave phenomena are predominant. The long-term objective is to provide model-based signal processing methods for the estimation and interpretation of the characteristics of these waves (shape, velocity), in order to assess the compartment function and the heart-compartment adaptation. As we have seen above, the PDE discretization approach leads to high order models for the Pressure Wave Transfer Function (PWTF). In what follow, the main idea to circumvent this problem will be to explicitly use a propagation delay, for example the Pulse Transit Time (PTT) that, in practice can be measured directly. A close look to the waves of interest leads to the hypothesis that they are indeed nonlinear waves. For example, during the travel of a pressure pulse from the heart towards a finger, it is easy to observe an increase of the pulse amplitude and a decrease of its width (peaking and steepening phenomena), at the opposite of what would be expected of linear weakly damped waves. Comparing the shapes of such pressure pulse wave, when it is close to the heart and when at the finger, it seems possible to interpret the downstream shape as a deformation of the upstream one due to higher velocities for higher peaks during the travel: this is particularly striking for the dichrotic wave. All these qualitative phenomena leads to consider the pulse wave as a solitary wave, for example generated by a Korteweg de Vries model for the flow. After this systolic phase a windkessel model will be able to represent the waveless phenomena as in [21]. These remarks are not new, but we want here to precise the corresponding computations, in particular the type of solitary waves, in order to be able to propose signal processing techniques. In a first part a quasi-1D Navier-Stokes equation is studied that takes into account a radial acceleration. The radial and axial acceleration terms being supposed very small and small respectively, a multiscale singular perturbation technique is used to isolate the fast wave propagation phenomena taking place in a boundary layer in time (and space) and the slow phenomena represented by a parabolic system similar to those studied for example in [12] or [9] and leading to two-elements windkessel models. For the hyperbolic system in the boundary layer, the situation is similar to

those leading to Korteweg de Vries equation when a direction of the solitary waves is chosen, which corresponds to the matching condition of the linear case. For example, using various asymptotic methods, Yomosa and Demiray [23, 3] studied the motion of weakly nonlinear pressure waves in a thin nonlinear elastic tube filled with an incompressible fluid. They proved that, when viscosity of blood is neglected, the dynamics are governed by the Korteweg-de Vries equation. We adapt this technique in the second part. In a third part we study particular solutions of the Korteweg-de Vries equation, namely the 2 and 3-soliton solutions that seem to be good candidates to match the observed pressure pulse waves. Finally we show the first comparisons of numerical results obtained along this line with real pressure data.

2 Asymptotic expansion of a quasi 1D model of flow : quasistatic approximation and KdV corrector.

In this section, we suppose that for normal space and time scales, the windkessel model predomines but, for small time and small space scales, there appears a boundary layer where the windkessel model is no more convenient. This ansatz is used in singular perturbation computations to develop a corrector of the motion of the fluid in this boundary layer.
The idea of a boundary layer where a corrector of the motion of the fluid satisfies a KdV equation is a conjecture to represent the wave phenomena rather fast when compared to the windkessel effect. We derive formally the equations satisfied by this corrector. We still need to prove that the solutions converge (in a sense to be defined) to the solutions of equations (1), (2), (3) and (4).
We suppose that the arteries can be identified with an elastic tube, and blood flow is supposed to be an incompressible fluid.
Thus, we consider a one dimensional elastic tube of mean radius R_0. The Navier Stokes equation can read as

$$A_T + Q_Z = 0, \tag{1}$$

$$Q_T + \left(\frac{Q^2}{A}\right)_Z + \frac{A}{\rho}P_Z + \nu\frac{Q}{A} = 0. \tag{2}$$

where, $A(T,Z) = \pi R^2(T,Z)$ is the cross-sectional area of the vessel, $Q(T,Z)$ is the blood flow and $P(T,Z)$ is the blood pressure. Moreover ρ is the blood density and ν a coefficient of viscosity of blood.
Furthermore, the motion of the wall satisfies, (see for example [23])

$$\frac{\rho_w h_0 R_0}{A_0} A_{TT} = (P - P_e) - \frac{h_0}{R_0}\sigma \tag{3}$$

where, ρ_w is the wall density, P_e is the pressure outside the tube, h_0 denotes the mean thickness of the wall. Moreover, σ is the extending stress in the tangential direction.

Remark 2.1 Usually the term $\frac{\rho_w h_0 R_0}{A_0} A_{TT}$ is neglected because A_{TT} is small. ◊

This system is completed by a model of the local compliance of the vessels, a state equation

$$\sigma = E\frac{\Delta A}{2A_0}. \tag{4}$$

where $\Delta A = A - A_0$, with A_0 the cross-sectional area at rest, and E is the coefficient of elasticity.
First of all, we rewrite system (1)-(4) in non dimensional variables.
Let

$$Z = Lz,\ T = \frac{L}{c_0}t$$

where L is the typical wave length of the waves propagating in the tube, $c_0 = \sqrt{\frac{Eh_0}{2\rho R_0}}$, with R_0 the means radius of the tube. The velocity c_0 is the typical Moens-Korteweg velocity of a wave propagating in an elastic tube, when all nonlinear terms are neglected. We suppose that $\epsilon = \left(\frac{R_0}{L}\right)^{2/5} << 1$. (For the arteries considered here, $\epsilon < 0,1$.)
Let us rescale pressure, blood flow and cross-sectional area by,

$$\begin{aligned} P - P_0 &= \rho c_0^2 p, \\ Q &= A_0 c_0 q, \\ A &= A_0(1+a), \end{aligned}$$

where A_0 and P_0 are the constant cross sectional area and the pressure at rest, ($P_0 = P_e$ the external pressure) and $Q_0 = 0$. Thus, we get the following system,

$$\begin{aligned} a_t + q_z &= 0, \\ q_t + \left(\frac{q^2}{1+a}\right)_z + (1+a)p_z &= -\frac{\nu L}{A_0 c_0}\frac{q}{1+a}, \\ \frac{\rho_w h_0 R_0}{\rho L^2} a_{tt} + a &= p. \end{aligned}$$

By hypothesis,

$$\frac{\rho_w h_0 R_0}{\rho L^2} = \frac{\rho_w}{\rho}\frac{h_0}{R_0}\frac{R_0^2}{L^2} = O(\epsilon^5) = \lambda\epsilon^5$$

Thus, we get,

$$a_t + q_z = 0, \tag{5}$$

$$q_t + \left(\frac{q^2}{1+a}\right)_z + (1+a)p_z = -\eta\frac{q}{1+a}, \tag{6}$$

$$\lambda\epsilon^5 a_{tt} + a = p. \tag{7}$$

We suppose that the solutions admit an asymptotic expansion in terms of ϵ,

$$a(t,z) = \sum_{k\geq 1} \epsilon^k a^k(\frac{t-z}{\epsilon^2}, \frac{z}{\epsilon}, t, z),$$
$$p(t,z) = \sum_{k\geq 1} \epsilon^k p^k(\frac{t-z}{\epsilon^2}, \frac{z}{\epsilon}, t, z),$$
$$q(t,z) = \sum_{k\geq 1} \epsilon^k q^k(\frac{t-z}{\epsilon^2}, \frac{z}{\epsilon}, t, z).$$

We perform the following change of variables,

$$\tau_1 = \frac{t-z}{\epsilon^2},\ \xi_1 = \frac{z}{\epsilon},\ \tau_2 = t,\ \xi_2 = z.$$

Remark 2.2 This change of variables implies that we consider only waves moving from left to right. If we keep both directions, we get a Boussinesq type model as for example in [15]. The validity of the approximations will be done a posteriori when comparing measured and computed data.
Remark also that we have chosen $\epsilon = \left(\frac{R_0}{L}\right)^{2/5}$ instead of $\epsilon = \frac{R_0}{L}$ as commonly done [2] so that the acceleration term in (7) does not disappear in the sequel. ♢

Thus equations (5)-(7) become (at the second order of ϵ),

$$\epsilon[a^1_{\tau_1} - q^1_{\tau_1}] + \epsilon^2[a^2_{\tau_1} + q^1_{\xi_1} - q^2_{\tau_1}] = 0, \tag{8}$$

$$\epsilon[q^1_{\tau_1} - p^1_{\tau_1}] + \epsilon^2[q^2_{\tau_1} - 2q^1q^1_{\tau_1} + p^1_{\xi_1} - p^2_{\tau_1} - a^1p^1_{\tau_1}] = 0, \tag{9}$$

$$\epsilon[a^1 - p^1] + \epsilon^2[\lambda a^1_{\tau_1\tau_1} + a^2 - p^2 = 0. \tag{10}$$

Thus, we get with (8)-(10),

$$a^1 = q^1, \tag{11}$$

$$q^1 = p^1, \tag{12}$$

$$2q^1_{\xi_1} - 3q^1q^1_{\tau_1} - \lambda q^1_{\tau_1\tau_1\tau_1} = 0. \tag{13}$$

In fast times, and in a boundary layer, q^1 is solution of a Korteweg-de Vries equation. In initial variables, we have the following KdV equation for the fast blood flow, $Q^1(T,Z) = A_0 c_0 q^1(\frac{c_0 T - Z}{L\epsilon^2}, \frac{Z}{L\epsilon})$, with (11)-(13)

$$Q^1_Z + d_0 Q^1_T + d_1 Q^1 Q^1_T + d_2 Q^1_{TTT} = 0, \tag{14}$$

with

$$\begin{aligned} d_0 &= \frac{1}{c_0} \\ d_1 &= -\frac{3}{2}\frac{1}{A_0 c_0^2}, \\ d_2 &= -\frac{\rho_w h_0 R_0}{2\rho c_0^3}. \end{aligned}$$

Remark 2.3 The blood pressure, P^1, and the cross sectional area ΔA^1 are also solutions of Korteweg-de Vries equations with some other parameters in the same boundary layer. ♢

Remark 2.4 Usually, with the available measurements (e.g. given by a FINAPRES sensor), we get the pressure as a function of time defined at a particular point, for example the finger. Thus, it is useful to get, not a time-evolution equation as usual, but a space-evolution equation as obtained in (14). ♢

The equation (14) describes rather fast travelling waves (3-10 m/s). After these waves have gone across the compartment there is still a slowly varying flow that will appear as some kind of parabolic flow well approximated by a windkessel model.

Indeed for large time or space, we neglect acceleration of blood flow, that is

$$A_T + Q_Z = 0, \tag{15}$$

$$\frac{A_0}{\rho} P_Z + \nu \frac{Q}{A} = 0, \tag{16}$$

$$\Delta P - \frac{h_0 E}{2A_0\rho_0}\Delta A = 0 \tag{17}$$

We get with (15)-(17) the following parabolic equation in Q,

$$Q_T - \frac{A_0 h_0 E}{2\rho\nu R_0} Q_{ZZ} = 0 \tag{18}$$

A low frequency approximation of (18) gives a 2 or 3 -element windkessel system, see for example [12, 13, 9].

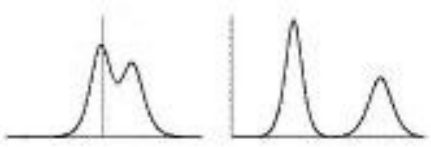

Figure 1: A 2-soliton solution at different positions

3 Modelling of pulsatile and non pulsatile blood flows.

After studying different pressure pulse waves measurements, an experimental finding was that the pulses can be approximated by 2-soliton or 3-soliton solutions of KdV. Roughly speaking a n-soliton, solution of the Korteweg-de Vries equation, see e.g. [8, 22], will have n components of different heights travelling with different velocities while interacting. See figure 1 for an example of a 2-soliton solution of KdV.
In the next two subsections, we give the analytical expression of these soliton solutions we will use in the sequel.

3.1 The 2-soliton pressure model

We know the analytical expression of a 2-soliton solution, see for example [22].
We first consider the following a-dimensioned KdV equation

$$y_\tau + 6yy_\xi + y_{\xi\xi\xi} = 0. \tag{19}$$

Then a 2-soliton solution of (19) can be written,

$$y(\tau,\xi) = 2\frac{a_1^2 f_1 + a_2^2 f_2 + (a_1-a_2)^2 f_1 f_2 + 2\left(\frac{a_1-a_2}{a_1+a_2}\right)^2 (a_2^2 f_1^2 f_2 + a_1^2 f_1 f_2^2)}{\left(1 + f_1 + f_2 + \left(\frac{a_1-a_2}{a_1+a_2}\right)^2 f_1 f_2\right)^2} \tag{20}$$

with

$$f_j(\tau,\xi) = \exp(-a_j(\xi - s_j - a_j^2\tau)),\ (a_j, s_j) \in \mathbb{R}^2 \text{ and } a_1 \geq a_2.$$

We perform the following change of variables,

$$\xi = T - d_0 Z,\ \tau = d_2 Z,\ Q^1(T,Z) = \frac{6d_2}{d_1} y(\xi,\tau).$$

Therefore, Q^1 is a solution of the blood flow KdV equation (14), and we have

$$Q^1(T,Z) = \frac{12d_2}{d_1} \frac{a_1^2 f_1 + a_2^2 f_2 + (a_1-a_2)^2 f_1 f_2 + 2\left(\frac{a_1-a_2}{a_1+a_2}\right)^2 (a_2^2 f_1^2 f_2 + a_1^2 f_1 f_2^2)}{\left(1 + f_1 + f_2 + \left(\frac{a_1-a_2}{a_1+a_2}\right)^2 f_1 f_2\right)^2} \tag{21}$$

$$\text{with } f_j(T,Z) = \exp(-a_j(T - s_j - Z(d_0 + a_j^2 d_2))) \, (a_j, s_j) \in \mathbb{R}^+ \times \mathbb{R}. \tag{22}$$

3.2 The 3-soliton pressure model

Following [22, pp 580], a 3-soliton solution of (19) is written $y(\tau,\xi) = 2(\ln\det A)_{\xi\xi}$, with A defined by

$$A = \begin{pmatrix} 1+f_1 & 2\frac{a_1}{a_1+a_2} f_1 & 2\frac{a_1}{a_1+a_3} f_1 \\ 2\frac{a_2}{a_1+a_2} f_2 & 1+f_2 & 2\frac{a_2}{a_2+a_3} f_2 \\ 2\frac{a_3}{a_1+a_3} f_3 & 2\frac{a_3}{a_2+a_3} f_3 & 1+f_3 \end{pmatrix}$$

and $f_j(\tau,\xi) = \exp(-a_j(\xi - s_j - a_j^2\tau))$.

Using the general formula,

$$y(\tau,\xi) = 2\frac{(\det A)_{\xi\xi} \det A - (\det A)_\xi^2}{\det A^2}.$$

The blood flow Q^1 solution of (14) is then given by

$$Q^1(T,Z) = \frac{12d_2}{d_1} y(T - d_0 Z, d_2 Z).$$

3.3 Identifiability of KdV coefficients.

Lemma 3.1. *If y_0 is the initial data of a n-soliton then ηy_0 is the initial data of a n-soliton (same n) if and only if $\eta = 1$.*

Proof: We prove this result in the 3 first cases, n=1, n=2 and n=3.

- Case n=1

  In that case, we have, $y_0(x) = \mathrm{sech}^2(x - s_0)$, and thus, ηy_0 is a 1-soliton if and only if $\eta = 1$.

- Case n=2

  In this subsection, we use the 2-soliton parameters of subsection 3.1.

  We look at the equivalent in time in $+\infty$ and in $-\infty$ of S a 2-soliton. By using Lamb formulae, [8], we get the following equivalents, by

letting a_1 and a_2 the 2 parameters of S (see formula (20)) with $a_2 < a_1$ and s_2 the initial time delay of the first component of the soliton.

$$S = 8\frac{a_1^2 - a_2^2}{(a_1 - a_2)^2} a_2^2 e^{2(a_2\xi + s_2)} \quad (+\infty) \tag{23}$$

$$S = 8\frac{a_1^2 - a_2^2}{(a_1 - a_2)^2} a_2^2 e^{-2(a_2\xi + s_2)} \quad (-\infty) \tag{24}$$

As ηS is supposed to be a 2-soliton it must have the same equivalent in time in $+\infty$ and in $-\infty$. Thus if we take b_1 and b_2 the 2 parameters of ηS with $0 < b_2 < b_1$ and r_2 the time delay, we get

$$8\eta\frac{a_1^2 - a_2^2}{(a_1 - a_2)^2} a_2^2 e^{2(a_2\xi + s_2)} = 8\frac{b_1^2 - b_2^2}{(b_1 - b_2)^2} b_2^2 e^{2(b_2\xi + r_2)}$$
$$8\eta\frac{a_1^2 - a_2^2}{(a_1 - a_2)^2} a_2^2 e^{-2(a_2\xi + s_2)} = 8\frac{b_1^2 - b_2^2}{(b_1 - b_2)^2} b_2^2 e^{-2(b_2\xi + r_2)}$$

We immediately deduce that $b_2 = a_2$, and $r_2 = s_2$ and we obtain the following equation,

$$\eta\frac{a_1 + a_2}{a_1 - a_2} = \frac{b_1 + a_2}{b_1 - a_2}$$

By using the first conserved quantity of the KdV solution (see Lamb [8]), for the 2-soliton solutions S and ηS, namely,

$$\int_{-\infty}^{+\infty} S(t, z)dt = C$$

we get,

$$\eta(a_1 + a_2) = b_1 + a_2$$

thus

$$a_1 = b_1, \quad \eta = 1$$

and we have exactly the same soliton.

- Case n=3

  In a first time, we rewrite the problem in the following form,
  $y_0 = \frac{\partial^2 \ln(\det(A_1))}{\partial x^2}$ and $\eta y_0 = \frac{\partial^2 \ln(\det(A_2))}{\partial x^2}$, where A_1 and A_2 are 3×3 matrices of the following form,

$$A_i = \begin{pmatrix} 1+\frac{m_1^i(0)}{2a_1^i}f_1^i & \frac{m_2^i(0)}{a_1^i+a_2^i}f_2^i & \frac{m_3^i(0)}{a_1^i+a_3^i}f_3^i \\ \frac{m_1^i(0)}{a_1^i+a_2^i}f_1^i & 1+\frac{m_2^i(0)}{2a_2^i}f_2^i & \frac{m_3^i(0)}{a_2^i+a_3^i}f_3^i \\ \frac{m_1^i(0)}{a_1^i+a_3^i}f_1^i & \frac{m_2^i(0)}{a_2^i+a_3^i}f_2^i & 1+\frac{m_3^i(0)}{2a_3^i}f_3^i \end{pmatrix} \tag{25}$$

with $f_j^i(\tau,\xi) = \exp(-a_j^i(\xi - s_j^i - (a_j^i)^2\tau))$.

Then, we want to know if there exist η, A_1 and A_2 in that form such that

$$\det(A_1)^\eta = \det(A_2) \tag{26}$$

We easily deduce from (25) that $\det(A_2)$ has at most 7 different exponential terms, that is

$$f_1^2,\ f_2^2,\ f_3^2,\ f_1^2f_2^2,\ f_1^2f_3^2,\ f_2^2f_3^2,\ f_1^2f_2^2f_3^2.$$

When we look at the equivalent series of $(\det A_1)^\eta$ in $+\infty$, we deduce that necessary, $\eta \in \mathbb{N}^*$.

Suppose in a first time that $\eta \geq 2$, then, $\det(A_1)^\eta$ has at least 8 different exponential terms, (with $a_1^1 > a_2^1 > a_3^1$)

$$f_1^1,\ f_2^1,\ f_3^1,\ f_1^1f_2^1f_3^1,\ f_1^1f_3^1,\ f_1^1f_2^1,\ (f_1^1f_3^1)^2,\ (f_1^1f_2^1f_3^1)^2.$$

Which is impossible, thus $\eta = 1$ and that ends the proof.

Theorem 3.2. *Suppose that for $Z = 0$ the pressure $P_0(T) = P^1(T,0)$ is known and is the initial data of a n-soliton (n known). Then for any other position $Z \neq 0$ $P^1(T,Z)$ is well defined and d_1 is identified as soon as we know the parameters d_0 and d_2.*

Proof: Thanks to Lemma 3.1, there exists one and only one η such that $\eta P_0(T)$ is the initial data of a n-soliton solution of the normalized KdV equation. But once the initial data of a KdV solution is known, this solution is unique and well known thanks to the inverse scattering method, see for example Lamb [8].

Remark 3.3 As $d_0 = (\rho d_1)^{1/3}$, and ρ is the density of the blood, we can expect this parameter constant for each patient, thus only d_2 needs to be known in theorem 3.2 $\Diamond$

Remark 3.4 The identifiability of the other parameters (the soliton ones) will be made in a forthcoming article [7]. $\Diamond$

3.4 Windkessel models and soliton correctors.

Following (2), we decompose blood pressure in a pulsatile and non pulsatile wave, i.e., a wave depending on time and space and a component depending only on time

$$P - P_0 = P^1(T, Z) + \hat{P}^1(T). \tag{27}$$

We already know the wave model, we still have to precise the windkessel model. We take a 2-element windkessel model. Let C be the compliance of the arterial tree and let R the resistance of the peripheral systemic circulation. Thus, we get (see [21]), with Q_{in} the inflow from the left ventricule.

$$\hat{P}^1(T) - P_\infty = (P_0 - P_\infty)e^{-\frac{T}{RC}} + e^{-\frac{T}{RC}} \int_{T_0}^{T} \frac{Q_{in}(t)}{C} e^{\frac{t}{RC}} dt. \tag{28}$$

We then need to identify the parameters coming from windkessel and soliton models.

3.5 Identifiability of pulsatile and non pulsatile blood pressure shapes and models.

In a first time we identify the parameters of the windkessel model, it is commonly believed that the pulsatile component is minimal during the last two-thirds of diastole, thus we can determine P_∞ and $\tau = RC$ from late diastolic shape.

We still have to determine the instant of onset and of offset of the disatole. With these 2 times, we have identified all the parameters of the windkessel component.

Thus, $P^1 = P - P_0 - \hat{P}^1$ is a 2 or 3 soliton and we can identify the parameters thanks to section 3.3.

4 Comparison of real pressure waves and windkessel-solitons representations.

4.1 A 2-soliton shape.

In figure 2, the 2-soliton is well adapted to represent the pressure pulse.

For the patient of figure 3, we don't need to correct the 2-soliton solution with a windkessel part. The heart rate is rather high after a tilt test, thus the windkessel effect doesn't appear.

4.2 A 3-soliton shape.

With a 3-soliton we obtain figures 4.

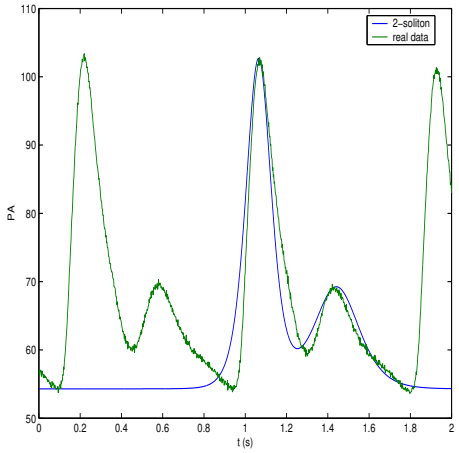

Figure 2: Pressure obtained with a FINAPRES sensor and superposed with a 2-soliton model

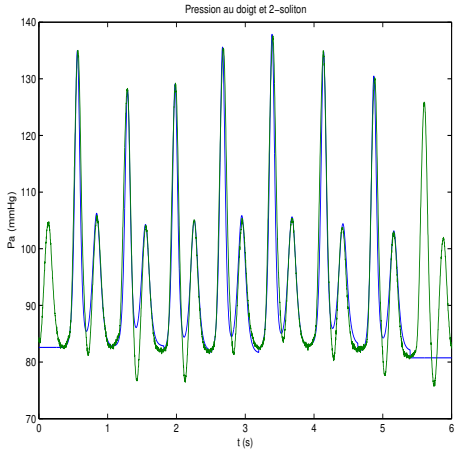

Figure 3: Pressure obtained with a FINAPRES sensor and superposed with a 2-soliton model after a tilt test

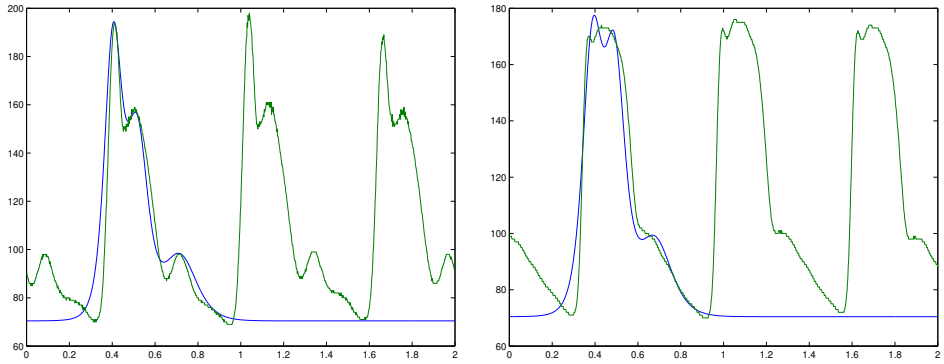

(a) (b)

Figure 4: 3-soliton model tuned with FINAPRES pressure (a). Estimated pressure at the catheter level compared with the measurement (b)

In 4(a), we have superposed a 3-soliton solution to a FINAPRES output. Then we have superposed the same soliton at $L = -0.4\,m$ with a radial pressure obtained with the same patient at the same time by using a catheter, figure 4(b).

4.3 A 2-windkessel-3-soliton shape.

With a 3-soliton we obtain the figures 5.

The figures 5 are obtained in the same way as figures 4.

Obviously, in figure 5, there is a windkessel part in the pressure pulse. In figure 6, we have superposed the pulse pressure measured at the end of finger, with a "3-soliton+windkessel" solution. The result obtained is better than in figure 5 but there is 4 more parameters to identify in that case.

5 Conclusion

In this article we have proposed a reduced model of the input-output behaviour of an arterial compartment, including the short systolic phase where wave phenomena are predominant. We believe that this model may serve as a basis for model-based signal processing methods for pressure estimation from non-invasive measurements and interpretation of the characteristics of pressure waves. The explicit use in the reduced model of nonlinear wave characteristics, among which some propagation delays, seems promising. Phenomena, such that peaking and steepening, are well taken into account by the soliton description. A first attempt is done here to separate the fast wave propagation phenomena taking place in a boundary layer in time and space described by a KdV equation from the slow windkessel effect repre-

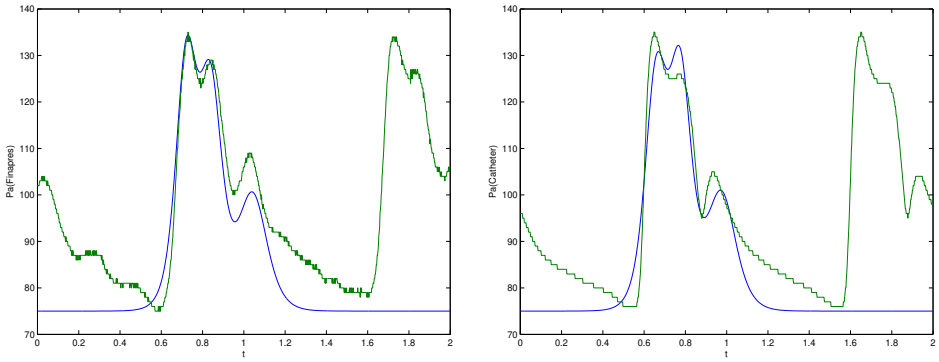

(a) (b)

Figure 5: 3-soliton model tuned with FINAPRES pressure (a). Estimated pressure at the catheter level compared with the measurement (b).

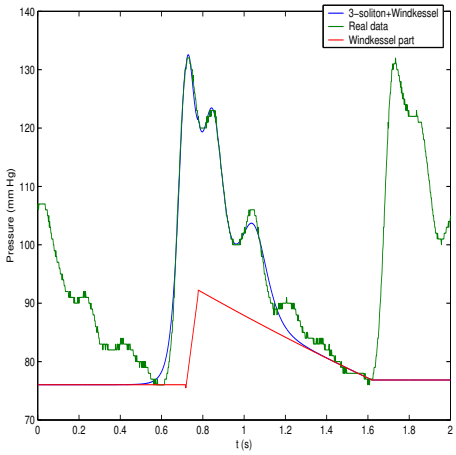

Figure 6: 3-soliton +windkessel representation of the pressure at the finger level

sented by a parabolic equation leading to windkessel models. It relies on the hypothesis that radial and axial acceleration terms are small. A heuristic multiscale singular perturbation technique is used to derive the model. Giving more solid basis to this technique will be the topics of further research. It is already possible to observe that 2 and 3-soliton descriptions of the waves combined with two-element windkessel models active outside a boundary layer, in the diastolic phase, lead to good experimental results to represent pressure pulse waves. The close form formulae of these nonlinear models of propagation in conjunction with windkessel models are rather easy to use to represent wave shapes at the input and output of an arterial compartment. Some very promising preliminary comparisons of numerical results obtained along this line with real pressure data have been shown.

Acknowledgment : The authors would like to thank Y. Papelier and hospital Béclère (Clamart) for providing us data obtained by simultaneously measuring FINAPRES output and catheterized radial pressure.

References

[1] Ayache, N., Chapelle, D., Clément, F., Coudière, Y., Delingette, H., Désidéri, J.-A., Sermesant, M., Sorine, M., and Urquiza, J. Towards model-based estimation of the cardiac electro-mechanical activity from egc signals and ultrasound images. In *Functional Imaging and Modeling of the Heart (FIMH 2001)* (Helsinki, Novembre 2001).

[2] Canic, S., and Mikelic, A. Effective equations modeling the flow of a viscous incompressible fluid through a long elastic tube arising in the study of blood flow through small arteries. *SIAM J. Applied Dynamical Systems 2* (2003), 431–463.

[3] Demiray, H. Nonlinear waves in a viscous fluid contained in a viscoelastic tube. *Z. angew. Math. Phys 52* (2001), 899–912.

[4] Franck, O. Die grundform des arteriellen pulses. *Erste Abhandlung, Mathematische analyse, Z. Biol. 37* (1899), 483–526.

[5] Hales, S. *Statical Essays containing Haemastatics: Or an Account of some Hydraulic and Hydrostatical Experiments made on the Blood and Blood-vessels of animals.* London: Innys and Mamby, 1733.

[6] Karamanoglu, M., and Feneley, M. On-line synthesis of the human ascending aortic pressure pulse from the finger pulse. *Hypertension 30* (1997), 1416–1424.

[7] Laleg, T., Crépeau, E., and Sorine, M. Separation of arterial pressure into solitary waves and windkessel flow. *In submission* (2006).

[8] Lamb, G. *Elements of soliton theory*. J. Wiley and sons, 1980.

[9] Milisic, V., and Quarteroni, A. Analysis of lumped parameter models for blood flow simulations and their relation with 1d models. *M2AN 4* (2004), 613–632.

[10] Millasseau, S., Patel, S., Redwood, S., Ritter, J., and Chowienczyk, P. Pressure wave reflection assessed from the peripheral pulse: is a transfer function necessary? *Hypertension 41* (2003), 1016–1020.

[11] Milnor, W. *Hemodynamics*. Baltimore, MD: Williams and Wilkins, 1989, pp. 42–47.

[12] Monti, A., Médigue, C., and Sorine, M. Short-term modelling of the controlled cardiovascular system. *ESAIM: Proceedings 12* (2002), 115–128.

[13] Olufsen, M., and Nadim, A. On deriving lumped models for blood flow and pressure in the systemic arteries. *Mathematical Biosciences and Engineering 1* (2004), 61–80.

[14] Ottesen, J. *General Compartmental Models of the Cardiovascular System. In Mathematical models in medicine*. Ottesen, J.T. and Danielsen, M. IOS press, 2000, pp. 121–138.

[15] Paquerot, J., and Remoissenet, M. Dynamics of nonlinear blood pressure waves in large arteries. *Physics Letters A 194* (1994), 77–82.

[16] Peskin, C. *Lectures on Mathematical Aspects of Physiology*, lectures in applied math. ed., vol. 19. F.C. Hoppensteadt, AMS, 1981.

[17] Quarteroni, A., and Veneziani, A. Analysis of a geometrical multiscale model based on the coupling of pde's and ode's for blood flow simulations. *SIAM J. on MMS 1* (2003), 173–195.

[18] Sainte Marie, J., Chapelle, D., and Sorine, M. Data assimilation for an electro mechanical model of the myocardium. In *Procceedings of European Medical and Biological Engineering Conference* (MIT, Boston, USA, 2003).

[19] Segers, P., Carlier, S., Pasquet, A., Rabben, S., Hellevik, L., Remme, E., backer, T. D., Sutter, J. D., Thomas, J., and Verdonck, P. Individualizing the aorto-radial pressure transfer function: feasibility of a model-based approach. *Am. J. Physiol. Heart Circ. Physiol. 279* (2003), 542–549.

[20] Stergiopulos, N., Westerhof, B., and Westerhof, N. Total arterial inertance as the fourth element of the windkessel model. *Am. J. Physiol. 276* (1999), 81–88.

[21] Wang, J., O'Brien, A., Shrive, N., Parker, K., and Tyberg, J. Time-domain representation of ventricular-arterial coupling as a windkessel and wave system. *Am. J. Physiol. Heart Circ Physiol 284* (2003), 1358–1368.

[22] Whitham, G. *Linear and nonlinear waves.* J. Wiley and sons, 1974.

[23] Yomosa, S. Solitary waves in large blood vessels. *J. of the Physical Society of Japan 56* (1987), 506–520.